FINAL REPORT

(2012-2015)

Development of Stimuli Responsive Polymeric Hydrogels and Their application

Sponsored by

Defense Research and Development Organization

(DRDO Sanction No: EPIR/ER/1103999M/01/1441)

Submitted by

S. K. Dolui, M. Boruah, B. J. Saikia

Dept. of Chemical Sciences

Tezpur University

Napaam-784028

Assam

October 2014

Preface

This project was started in the month of October, 2012. It was my pleasure to work in the project. I am quite satisfied with the progress of the work. This report includes the progress of the project entitled "Development of Stimuli Responsive Polymeric Hydrogels and Their application". I am grateful to DRDO for sponsoring the project, I am also thankful to Tezpur University for allowing to carry out the project work.

S. K. Dolui

Principal Investigator

Achievements in Brief

(1) Electrical Actuation of electro-responsive hydrogels based on poly (acrylamide -co-acrylic acid)/Graphite suitable for biomedical applications:

- Synthesis and characterizations of conducting hydrogel based on poly(Acrylamide-co-Acrylic acid) and graphite.
- The structures of the hydrogels were confirmed and the influences of crosslinker and graphite content on the conductivity of the hydrogel were investigated.
- The actuation behaviour of the prepared hydrogels was determined.

(2) Synthesis and evaluation of swelling kinetics of electric field responsive Poly (vinyl alcohol)-g-polyacrylic acid/OMMT nanocomposite hydrogels:

- Nanocomposite hydrogels of PVA, partially neutralized acrylic acid and layered organically modified OMMT clay were prepared by free radical graft polymerization reaction.
- Introduction of OMMT to the polymer network results in an increase in thermal stability.
- The nanocomposite hydrogels showed significant and quick bending towards the cathode under the application of electric field.

(3) Electric Field Assisted Drug Release from pH and electro-responsive Gelatin-*g*-poly(acrylic acid)/MWCNTs nanocomposite hydrogels:

- Synthesis of pH and electro-responsive Gelatin-g-poly(acrylic acid)/MWCNTs nanocomposite hydrogels.
- The nanocomposite hydrogels were characterized by FTIR, SEM, TEM and XRD analysis.
- The effects of pH, MWCNT-COOH content and applied electric field on swelling behaviour of the hydrogels were determined.
- Electric Field Assisted Drug Release from the prepared nanocomposite hydrogels has been studied with respect to various parameters.

Details of the work done

(a) Electrical Actuation of electro-responsive hydrogels based on poly (acrylamide -co-acrylic acid)/Graphite suitable for biomedical applications:

1. Experimental

1.1 Materials

Acrylic acid (AA) was purchased from Merck Limited (Mumbai, India) and purified by vacuum distillation at 55°C. Acrylamide, tetramethylethylenediamine (TEMED) and graphite powder were purchased from Aldrich and were used as received. Potassium persulphate (KPS), as an initiator, supplied by Merck and was recrystallized before use. Di-sodium phosphate (Na_2HPO_4) and potassium hydrogen phosphate ($KHPO_4$) were purchased from Merck. Other chemicals such as hydrochloric acid, ethylene glycol dimethylacrylate (EGDMA) were also of analytical grade and used without any further purification.

1.2 Fabrication of Poly(AAm-co-AAc)/graphite conducting hydrogel

A polymer matrix composed of poly(acrylamide-co-acrylic acid)/graphite was prepared by dissolving a predetermined amounts of acrylamide, acrylic acid monomer in distilled water. Subsequently, graphite micropowder was dispersed in the above solution thoroughly to form a mixed solution. A given amount of crosslinker ethylene glycol dimethacrylate (EGDMA) was dissolved in the monomer/graphite mixed solution and the whole mixture was ultrasonicated for 30 minutes. The redox initiator system potassium persulfate (KPS) and N,N,N′,N′-tetraethylmethylendiammine (TEMED) were added to the mixture under stirring condition. The homogenized mixture was kept in a petridish for 24 hours. On completion of the reaction, the entire mass got converted into a dark black film which was then purified by equilibrating the film in double distilled water for a week. The swollen gel was dried at room temperature, cut into rectangular pieces and stored in airtight plastic bags.

2. Characterization tools and methods:

To gain insights into the structural information of prepared hydrogels, the IR spectra of the hydrogels were recorded with a Nicolet Impact-410 IR spectrometer (USA) in KBr medium at room temperature in the region 4000–450 cm^{-1}. The surface morphology of the composites was observed using a scanning electron microscope (SEM) (Model- JSM-6390LV, JEOL, Japan). The surface of the sample was platinum coated before SEM analysis.

2.1 Electrical Conductivity

The electrical conductivities of hydrogels were measured using four probe technique in the temperature range $300K \leq T \leq 413K$. The electrical conductivity of the composites were calculated using the following relation-

$$\rho = (V/I)\, 2\pi S,$$

where ρ is the resistivity of the sample, V is the applied voltage, I is the measured current through the sample and S is the distance between probes. Current-voltage (I-V) characteristics of prepared samples were recorded with a Keithley 2400 source meter at room temperature within the frequency range 102–106 Hz.

2.2 Swelling properties

To measure the degree of swelling the hydrogels, dried samples were placed in buffer media of different pH values at room temperature until the hydrated gels reached a stable weight. The water absorbed on the surface of the hydrogels was removed using filter paper and the weight noted.

$$\text{Swelling \%} = \frac{W_s - W_{dry}}{W_{dry}} \times 100$$

Where, W_s is the weight of the hydrogels in swollen state and W_{dry} is that of the hydrogels in dry state.

2.3 Actuation

The bending angle of the gels under applied electric fields was measured using a self developed device as shown in Fig. 1. To demonstrate the bending behaviour of the hydrogels, the two carbon electrodes were placed in parallel 30mm apart. One end of the sample column was fixed and placed vertically between two carbon electrodes in aqueous NaCl solution and the bending behavior was investigated under an applied electric field.

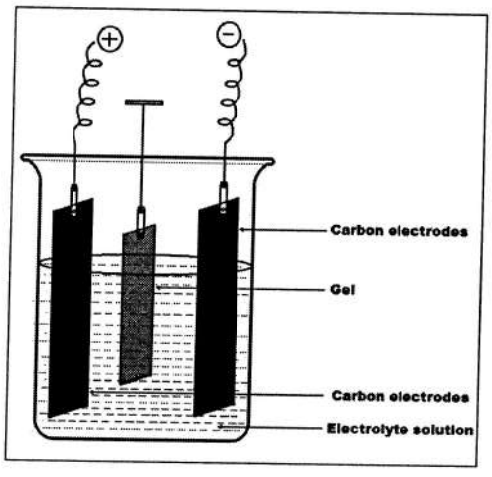

Fig.1 Apparatus for measuring bending angle.

3. Results and Discussions

3.1 FTIR analysis

FT-IR analysis was carried out to elucidate the composition of the hydrogel and spectra are shown in the Fig. 2. FT-IR spectrum of the hydrogel shows peaks at 3468, 3410, 3185, 2925, 1726, 1630, 1437, 1266 and 442 cm^{-1}. The characteristic peak at 3468 cm^{-1} is assigned to the O-H stretching from carboxylic group. Peak at 3410 cm^{-1} is due to N-H stretching vibration, at 3185 cm^{-1} is due to N-H bending vibration from $-CONH_2$ group of PAAm. Also, the characteristic peaks at 1726 cm^{-1} is due to C=O stretching of carboxylic acid group of PAA and 1630 cm^{-1} is for C=O stretching of PAAm. Peak at 1437 cm^{-1} is due to the aromatic C=C stretching vibration, 1266 cm^{-1} is due to the C-N stretching vibration and at 442 cm^{-1} is due to the $-NH_2$ out of plan rocking. The results indicate the formation of poly(AAm-*co*-AAc) hydrogel.

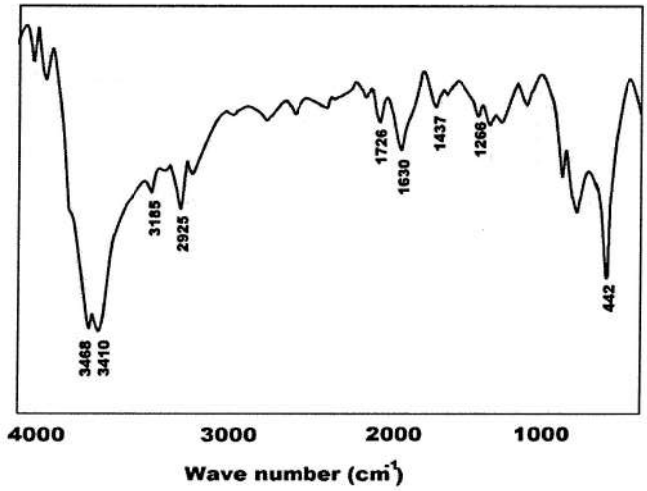

Fig.2 FTIR spectra of graphite impregnated gel.

3.2 SEM morphological observation

Fig. 3 illustrates the scanning electron micrographs of poly(AAm-*co*-AAc) copolymer hydrogel with and without graphite. The surface morphology of the hydrogel without graphite appears to be rough while with graphite it is found to be smooth. Here, the graphite particles may act as nucleating centre over which polymer grows with uniform rate.

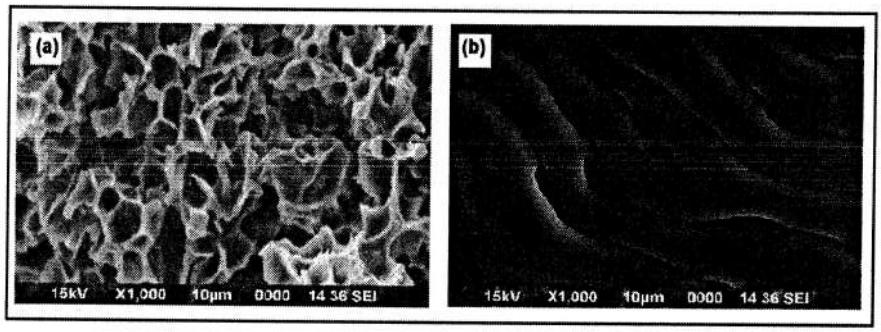

Fig.3 SEM images of (a) poly(AAm-*co*-AAc) gel and (b) graphite impregnated gel.

3.3 Influence of crosslinker concentration on the conductivity of hydrogel

The structure of the polymeric network plays a significant role in the electrical conductivity of hydrogel. The conductivity tends to increase initially with increase of crosslinker (EGDMA) amount from 0.03-0.09 mol% and again decreases beyond a crosslinker amount of 0.10 mol% as shown in the Fig. 4. Initial increase in amount of crosslinker facilitates the formation of a proper network structure which in turn enhances the uniformity in distribution of graphite into the hydrogel matrix. So the conductivity increases with increasing amount of crosslinking agent. Again, beyond an optimum level of crosslinker amount, the network becomes compact restraining the mobility of the charge carriers. So, at higher crosslinking density, the connection between graphite particles decreases thereby decreasing the electrical conductivity of the hydrogel.

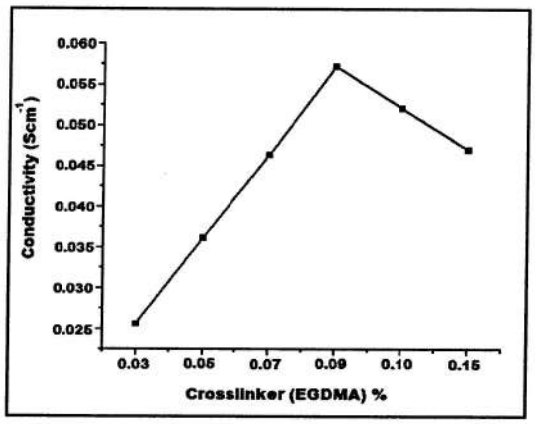

Fig.4 Conductivity with the variation of crosslinker amount.

3.4 Influence of graphite amount on the conductivity of hydrogel

Fig.5 represents the conductivities of the prepared hydrogels with the variation of graphite amount. The electrical conductivity of the prepared hydrogels is mainly accounted for the presence of graphite micropowder component. It was observed that the conductivity values increases with the increase in graphite content from 3 to 9 w%. With the increase of graphite

amount, the contact between the graphite particles increase which leads to the enhancement of conductivity. On the other hand, conductivity tends to decrease when amount of graphite exceeds 9 w%. It may be due to the fact that, with increase in amount, graphite particles tend to form agglomerates thereby restricting the uniform distribution of graphite within the hydrogel matrix. So, a little decrease in the conductivity value was observed.

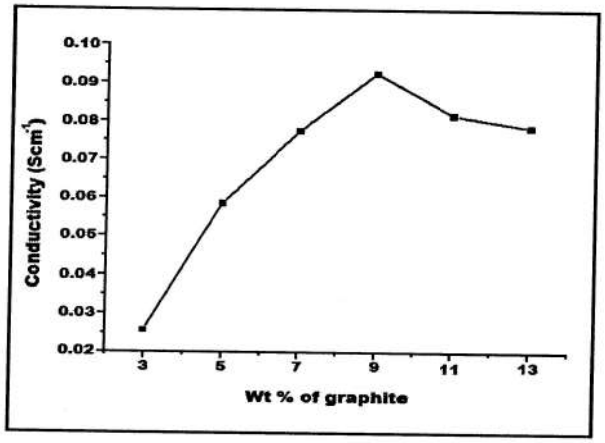

Fig.5 Conductivity with the variation of graphite amount.

3.5 Swelling behavior

The swelling behavior of hydrogels is a measure of their utility as biomaterials in various fields. So, the swelling behaviors of the composite hydrogels without graphite and with graphite are investigated and shown in Fig. 10 & 11. In both the cases, swelling behaviours are found to be same, but the values tend to decrease slightly with incorporation of graphite into the hydrogel matrix. It may be due to the hydrophobic nature of the graphite molecules present within the hydrogel matrix.

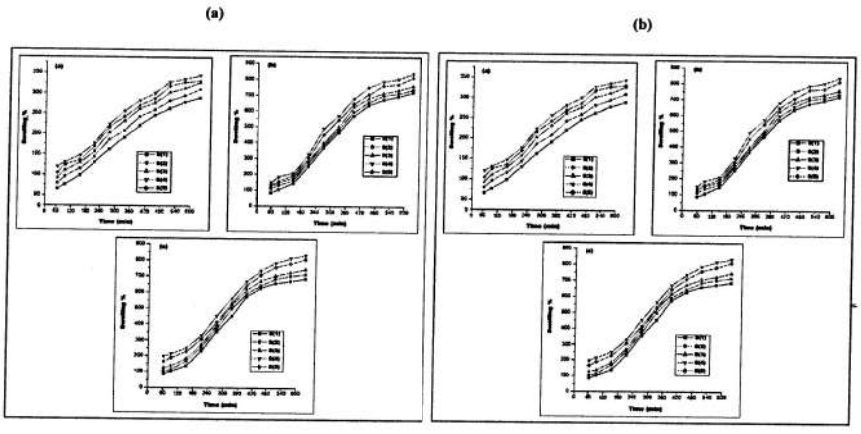

Fig.6 Swelling % of the hydrogels (i) without graphite and (ii) with graphite in different pH medium: (a) pH 4, (b) Distilled water and (c) pH 7.4.

The hydrogels were allowed to swell in different pH media. The swelling percentage is found be highest in basic medium (higher pH). With diminishing acidity of the media (higher pH), ionization of the carboxylic acid groups occurs, resulting in both electrostatic repulsion between the carboxylate (–COO^-–) groups as well as expansion of the space network.[1] Also, there is development of a large osmotic swelling force caused by the presence of the ions.

Furthermore, presence of crosslinker is an important pre-requisite for formation of ideal three-dimensional networks of hydrogels. Under lower crosslinker concentrations, the 3D network of the polymer does not form effectively in the gel. Thereby 3D network of gel cannot hold sufficient water which leads to decrease in swelling percentage. So, as the amount of crosslinker increases, the 3D network of the polymer forms effectively. After an optimum level of crosslinker amount, the network density increases which results in a compact network causing decrease in swelling.

3.6 Actuation behaviour

When an electric field was applied to a strip of the hydrogel in an aqueous NaCl solution, the hydrogel showed significant and quick bending towards the anode. When the electric stimulus was removed, it returned to its original position. The bending behavior of the hydrogels under varying concentrations of the electrolyte solution and applied voltages are shown in Fig. 7. It is clear that the bending angle is low when applied voltage is low and tends to increase with increase in applied voltage. The increase in effective bending angle may be attributed to the fact that with increase in voltage, the charged matrix is attracted more and more towards the electrodes leading to the said observation. However, bending was not found in pure water and this indicates that bending was induced by the electric current.[2] The effect of voltage on bending phenomenon has been investigated in the range 3.0 to 12.0 V. No bending was observed below 3.0V; so, lower critical voltage (LCV) found in this case is 3.0volt.

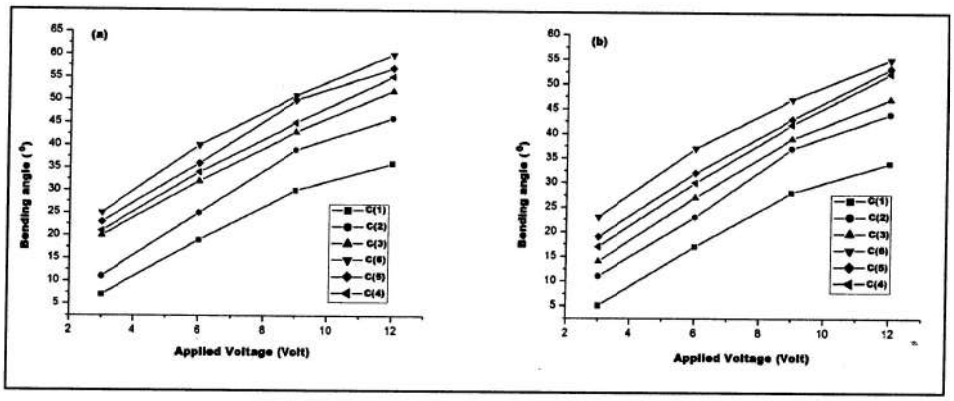

Fig.7 Effective bending angles of the hydrogels, (a) in 0.1N NaCl solution and (b) in 0.2N NaCl solution.

The influence of the medium ionic concentration on the bending behavior of the hydrogel in response to an electric stimulation was determined by varying the concentrations of aqueous

NaCl from 0.1and 0.2 N separately. It was found that bending angle tends to decrease at higher concentrations of the electrolyte. This may be due to the fact that beyond a critical electrolyte concentration, the ions present in the polymer chain are shielded by the other ions in the electrolytic solute which leads to the electrostatic repulsion of the polyions and a decrease in the degree of bending.[3] Also, according to Flory's theory, an increasing amount of ions could reduce the electrostatic repulsion of the polyions by the screening of fixed charges and bring about a decrease in the degree of bending. So, bending angles are found to decrease with increase in electrolyte concentration.[4]

4. Conclusion

In summary, we have demonstrated a simple method for the synthesis of poly(AAm-*co*-AAc) hyhrogels impregnated with graphite via aqueous polymerization. The FTIR spectrum shows the characteristic peaks of the functional groups of constituent polymers. The impregnation of graphite into the polymer matrix was confirmed by SEM analysis. The swelling properties of the prepared hydrogels were found to be pH responsive upon study across varying pH media. Swelling percentage was found to be good across all tested media, the highest being in basic medium. The hydrogels show significant bending behaviour when exposed to an external electric field. From this, it can be concluded that the hydrogels are sensitive to pH and electric field.

(b) Synthesis and evaluation of swelling kinetics of electric field responsive Poly (vinyl alcohol)-g-polyacrylic acid/OMMT nanocomposite hydrogels:

1. Materials

1.1 Experimental

Acrylic acid monomer (Aldrich) was distilled under reduced pressure prior to use. PVA, potassium persulfate (I, initiator), glutaraldehyde as a crosslinking agent, MMT nanoclay, and N, N, N', N'- tetramethylethylene diamine were supplied by Aldrich (A.R. grade). CTAB was supplied by G.S Chemical testing lab & allied industries, New Delhi. Sodium hydroxide and ethanol were purchased from Merck and were of A. R grade.

1.2 Fabrication of PVA-g-PAA/OMMT nanocomposite hydrogels

1.2.1 Preparation of organo-MMT nanoclay

The organophilic clay was prepared by treating the clay with CTAB as reported elsewhere.[5] 3g clay (Na^+-MMT) was dispersed in 250ml of deionized water under vigorous stirring (700rpm). A solution of CTAB (1.318g, 3.615x 10^{-3} mol) in 100ml of deionized water was slowly added to the dispersion, under continuous stirring. The resultant dispersion was stirred for a further

6hours. The dispersion was filtered and obtained cake was thoroughly washed with deionized water. Samples of the filtrate were taken in regular intervals and tested with a solution of 0.1 M silver nitrate for the presence of released counterions. Washing was discontinued only when the filtrate did not give a positive test to silver nitrate. The washed cake was dried overnight under reduced pressure (vacuum) at 40^0C and ground in a mortar.

1.2.2 Preparation of PVA-g-PAA/OMMT nanocomposite hydrogels

Poly(vinyl alcohol)-g-polyacrylic acid /OMMT nanocomposite hydrogels were prepared by free radical polymerization in distilled water. Before polymerization, 2 g of PVA was dissolved in 30 ml of hot double distilled water. Partially neutralized (60%) acrylic acid monomer was added to the PVA solution. Also, a certain amount of OMMT nanoclay was immersed in the deionized water for 2 h and dispersed under the ultrasonic vibration for 30 min. Both the solutions were mixed well and subsequently, glutaraldehyde (0.3-1.5 mol%), potassium persulfate (0.18mol%) and TEMED (0.05mol%) were added to the mixture under continuous stirring. Nitrogen was used to remove dissolved oxygen from the reactive solution. The reactive solution was first prepolymerizd at 70^0C for 30 min under stirring, and then poured into a petri dish quickly. The post polymerization was carried out at 65^0C for 15 h. When the reaction completed, the hydrogel was cut into same size and immersed in repeatedly changed deionized water for 72 h to remove the residual monomers. Table 1-2 outline the feed compositions of subsequently prepared hydrogels

Table 1. Compositions of PVA-g-PAA/OMMT nanocomposite hydrogels with various crosslinker (Glutaraldehyde) content:

Ingredients/Sample	**G(1)**	**G(2)**	**G(3)**	**G(4)**	**G(5)**	**G(6)**
PVA(g)	2	2	2	2	2	2
Acrylic Acid (ml)	1.5	1.5	1.5	1.5	1.5	1.5
OMMT (wt%)	1	3	5	7	9	11
KPS (mol%)	0.18	0.18	0.18	0.18	0.18	0.18
Glutaraldehyde (mol%)	0.9	0.9	0.9	0.9	0.9	0.9
TEMED (mol%)	0.05	0.05	0.05	0.05	0.05	0.05

Table 2. Compositions of PVA-*g*-PAAc/OMMT nanocomposite hydrogels with various OMMT nanoclay content:

Ingredients/Sample	S(1)	S(2)	S(3)	S(4)	S(5)	S(6)	S(7)
PVA(g)	2	2	2	2	2	2	2
Acrylic Acid (ml)	1.5	1.5	1.5	1.5	1.5	1.5	1.5
OMMT (wt%)	5	5	5	5	5	5	5
KPS (mol%)	0.18	0.18	0.18	0.18	0.18	0.18	0.18
Glutaraldehyde (mol%)	0.3	0.5	0.7	0.9	1.2	1.3	1.5
TEMED (mol%)	0.05	0.05	0.05	0.05	0.05	0.05	0.05

1.3 Characterization tools and methods

1.3.1 Fourier transform infrared spectrometer (FTIR)

To gain insights into the structural information of prepared hydrogels, the IR spectra of the hydrogels were recorded with a Nicolet Impact-410 IR spectrometer (USA) in KBr medium at room temperature in the region 4000-450 cm^{-1}.

1.3.2 X-ray diffraction (XRD) study

Powder X-Ray diffraction (XRD) data were collected on a Rigaku Miniflex X-ray diffractometer (Tokyo, Japan) with Cu Kα radiation (λ=0.15418 Å) at 30 kV and 15 mA with a scanning rate of $0.05^{o}s^{-1}$ in a 2θ ranges from 10°-70° for the native gel and 0-45° for OMMT nanoclay and nanocomposite hydrogel.

1.3.3 Scanning Electron Microscopy (SEM)

The surface morphology of the composites was observed using a scanning electron microscope (SEM) (Model- JSM-6390LV, JEOL, Japan). The surface of the sample was platinum coated before SEM analysis.

1.3.4 Swelling kinetics

The swelling capacity of a hydrogels can be determined by the amount of space inside the hydrogels network available to accommodate water. Three forces; polymer–water interactions, electrostatic and osmosis expand the hydrogels network to accommodate water inside it. The maximum amount of water that can be absorbed by a hydrogel is called its 'equilibrium swelling capacity' which depends on many factors including hydrogel structure, crosslinking density, ionic content and hydrophilic content. The suitability of hydrogels as biomedical materials and their performance in a particular application depend to a large extent on their bulk structure. Three important parameters can define the structure of a hydrogel, the polymer volume fraction in swollen state $v_{2,s}$, the number average molecular weight between the crosslinks (M_c) and the correlation length (ξ).[6]

In our work, the polymer volume fraction of the hydrogel in swollen state $v_{2,s}$ was estimated using the equation:

$$v_{2,s} = v_d/v_s \qquad (1)$$

where, V_d is the polymer volume fraction in dry state and V_s is the polymer volume fraction in swollen state. The value of V_d and V_s are determined by using the buoyancy principle with equation (2) and (3) as follows:

$$V_d = m_a\text{-}m_h/\rho_h \qquad (2)$$

$$V_s = m_{a,s}\text{-}\, m_{h,s}/\rho_h \qquad (3)$$

where, m_a is the mass of the initially dry polymer in air, m_h is the mass of the dry polymer in n-heptane, $m_{a,s}$ is the mass of swollen hydrogel in air after reaching equilibrium swelling, $m_{h,s}$ is the mass of swollen hydrogel in n-heptane after reaching equilibrium swelling and ρ_h is the density of n-heptane (0.684 g/cm^3 at 37±0.1°C). Prepared hydrogels were weighed in air and in n-heptane where a brass wire (0.04 mm in diameter) basket was suspended for placing samples.

1.3.5 Effective molecular weight of the polymer chain between two neighbouring crosslinks, $\overline{M_c}$

The molecular weight between two consecutive crosslinks, which can be either chemical or physical in nature, is a measure of the degree of crosslinking of the polymer. But due to the random nature of the polymerization process only average values of $\overline{M_c}$ can be calculated. Based on the equilibrium swelling data, effective molecular weight of the polymer chain between two neighbouring crosslinks, M_c was calculated using equation:[7]

$$\frac{1}{\overline{M}c} = \frac{2}{\overline{M}n} - \frac{\left(\frac{\bar{v}}{V_1}\right)\left[\ln(1-v_{2,s}) + v_{2,s} + \chi_{12} v_{2,s}^2\right]}{v_{2,s}^{1/3} - \frac{v_{2,s}}{2}} \quad (4)$$

Where, $\overline{M_n}$ is the number average molecular weight of PVA before crosslinking and taken as 1,25,000. $\bar{\upsilon}$ is the specific volume of PVA before crosslinking and was taken as 0.788 cm^3/g,[8] V_1 is the molar volume of the solvent (water) - 18 cm^3mol^{-1}.$\upsilon_{2,s}$ is the polymer volume fraction in swollen state and was calculated using equation (1). The value of Flory Huggins polymer water interaction parameter equal to 0.494.

1.3.6 Mesh size, ξ

An important structural parameter for analyzing hydrogels is the space available between macromolecular chains. This space is often regarded as the molecular mesh or pore which is denoted by ξ. Also, it can be reported only as an average value. Using the calculated values of number average molecular weight between crosslinks, mesh size for size for the hydrogel was estimated using equation (5):

$$\xi = \upsilon_{2,s}^{-1/3} \left[C_n(2M_c/\overline{M_r})\right]^{1/2} .\ell \quad (5)$$

Where, C_n is the Flory characteristics ratio for PVA = 8.3, ℓ is the carbon-carbon bond length along the polymer backbone which is equal to 1.54 Å, M_r is the average molecular weight of the repeating units of PVA and acrylic acid in $gmol^{-1}$.

1.3.7 Bending-Angle Measurement under electric field

Bending angle measurement was carried out under the noncontact dc electric field. For this, PVA-g-PAA/OMMT hydrogels were swollen in different concentrations of aqueous NaCl solution at room temperature and cut into 20×5×0.4 mm rectangular pieces. Then the bending angle of the gels under applied electric fields was measured using a self developed device as shown in Fig. 1. To demonstrate the bending behaviour of the hydrogels, the two carbon electrodes were placed in parallel 30mm apart. One end of the sample column was fixed and placed vertically between two carbon electrodes in aqueous NaCl solution and the bending behavior was investigated under an applied electric field.

1.4 Results and discussion

1.4.1 FTIR analysis

FTIR spectra of OMMT nanoclay, PVA-g-PAA copolymer and PVA-g-PAA/OMMT nanocomposite hydrogels were recorded to investigate the formation of the nanocomposite as shown in Fig. 8 (a, b & c). The FTIR spectrum of OMMT nanoclay shows characteristics peaks at 3631 cm^1, -OH stretching; 1637 cm^{-1}, -OH bending; 1108 cm^{-1}, Si-O stretching (out-of-plane);

1044 cm^{-1}, Si-O stretching (in-plane); 830 cm^{-1}, Al-Mg-OH bending vibrations and at 522 cm^{-1} due to the bending vibrations of Si-O. Also, the characteristics peaks were found for PVA-g-PAA copolymer at 1730–1850 cm^{-1} due to the presence of C=O stretching vibration and the peak observed at 639 cm^{-1} is due to the -OH out of plane vibration of the carboxylic groups of PAA, which obviously confirms the grafting reaction. The characteristic peaks at 3468 cm^{-1} and 3420 cm^{-1} are due to -OH stretching vibration of PVA and PAA, respectively, which also confirms the grafting of PAA into PVA. Other characteristics peaks for PVA are found at 2890 cm^{-1} for $-CH_2$ stretching, 1402 cm^{-1} for –O=C-OR stretching and at 860 cm^{-1} for –CH stretching vibrations respectively.

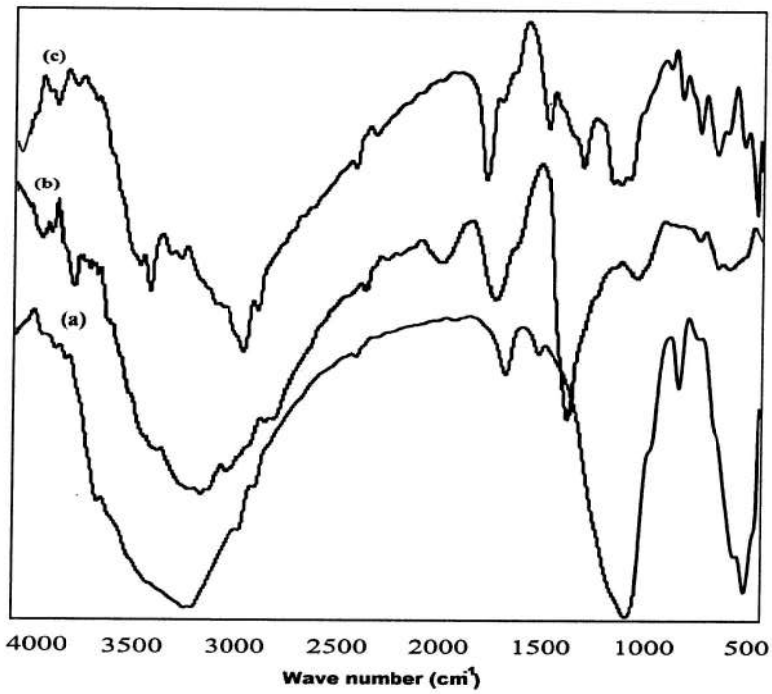

Fig.8 Representative FT-IR spectra of (a) OMMT nanoclay, (b) PVA-g-PAA copolymer and (c) PVA-g-PAA/OMMT nanocomposite hydrogel.

From the FTIR spectrum of PVA-g-PAA/OMMT nanocomposite hydrogel, it was found that, characteristics peaks occur at 1735-2010 cm^{-1} due to the presence of C=O stretching vibration, 3600-3450 cm^{-1} due to -OH stretching vibrations. Also, peaks at 1050 -1000 cm^{-1} are found which are the characteristics peaks for OMMT nanoclay. When OMMT nanoclay was incorporated into the PVA-g-PAA gel matrix, it was observed that peaks intensity related to PVA-g-PAA gel have increased. So, it can be said that OMMT nanoclay is acting here as active fillers.

1.4.2 XRD analysis

XRD experiments were run to gather information on the structure of PVA-g-PAA/OMMT nanocomposite hydrogel and Fig. 9 shows the XRD spectra of the native gel and Fig. 10 (a, b)

represents that of the OMMT nanoclay and the nanocomposite hydrogel respectively. A prominent peak is observed near 19.4° (d-spacing of 4.57A°) in the XRD spectrum of PVA-g-PAA, which corresponds to the (101) plane of the PVA crystal. Other minor peaks around 21 and 22° could be attributed to minor crystallites of grafted polyacrylic acid chains. Pure OMMT displays a diffraction peak at 6.24°, corresponding to a d-spacing of 14.12A°. But after incorporation of 3.0 wt% of the mineral clay (OMMT) in the polymer matrix, a peak at 4.69° corresponding to a d-spacing of 18.6A° was found. This increase in d-spacing indicates the increasing of layers spacing due to the intercalation or exfoliation of organophilic clay into the PVA-g-PAA copolymer matrix.

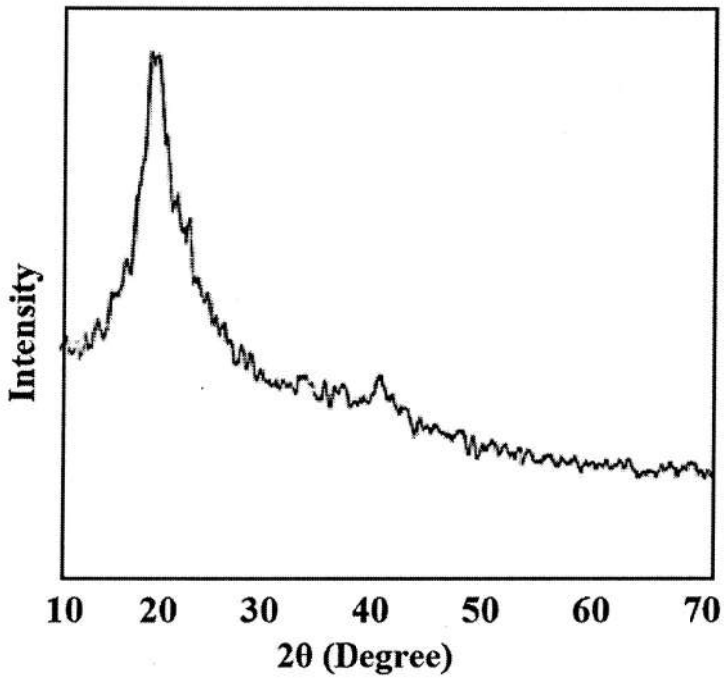

Fig. 9 XRD pattern of PVA-g-PAA copolymer hydrogel.

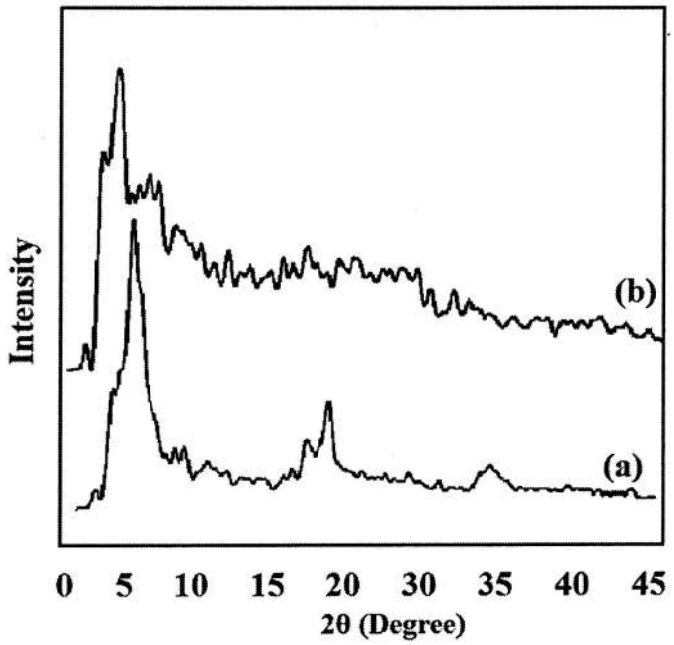

Fig. 10 XRD patterns of (a) OMMT nanoclay and (b) PVA-g-PAA/OMMT nanocomposite hydrogel.

1.4.3 SEM analysis

One of the most important properties that must be considered is hydrogel composite microstructure morphologies. The morphological image of the nanocomposite hydrogel was studied by SEM. The SEM images in Fig. 10 show that the morphology of PVA-g-PAA/OMMT becomes smoother than pure polymer. Also, the clay incorporated hydrogel matrix is found to be filamentous. Since PVA is crystalline in nature. So, this morphological change can be attributed to the re-ordered crystalline phase of the PVA matrix, causing a packed network.

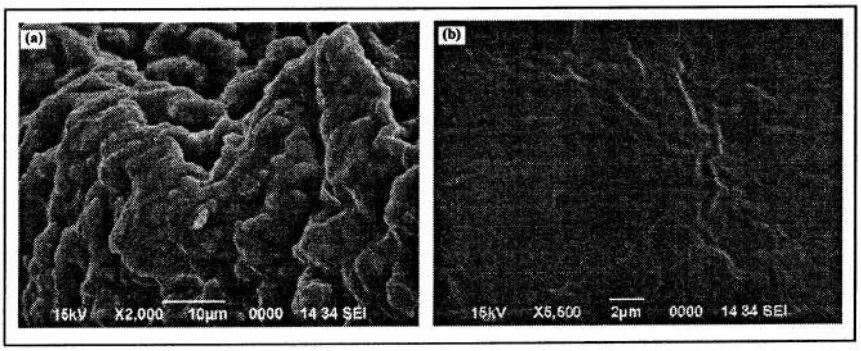

Fig.11 SEM micrographs of (a) PVA-g-PAA hydrogel and (b) PVA-g-PAA/OMMT nanocomposite hydrogel.

1.4.4 Swelling behaviour

The swelling behavior of hydrogels is a measure of their utility as biomaterials in various fields. Fig. 12 represents the swelling behaviour of the composite hydrogels with the variation of crosslinker and with different OMMT content as a function of time, from which some differences can be observed.

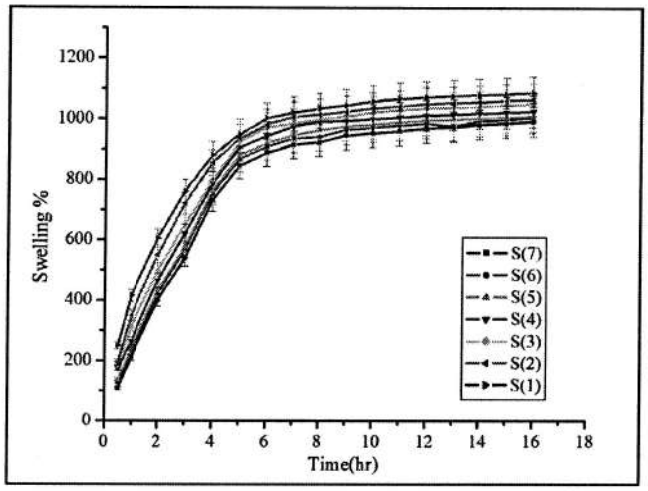

Fig.12 Swelling curves of PVA-g-PAA/OMMT nanocomposite hydrogel with various crosslinker amounts.

It was observed that the water absorbency decreased with the increase of clay content. It may be due to the fact that, inorganic clay mineral particle in network acted as an additional network point. The crosslinking density of composite increased with the increase of OMMT content, which resulted in a decrease in water absorbency. Fig. 13 represents the influence of clay amount on swelling behaviour of the nanocomposite.

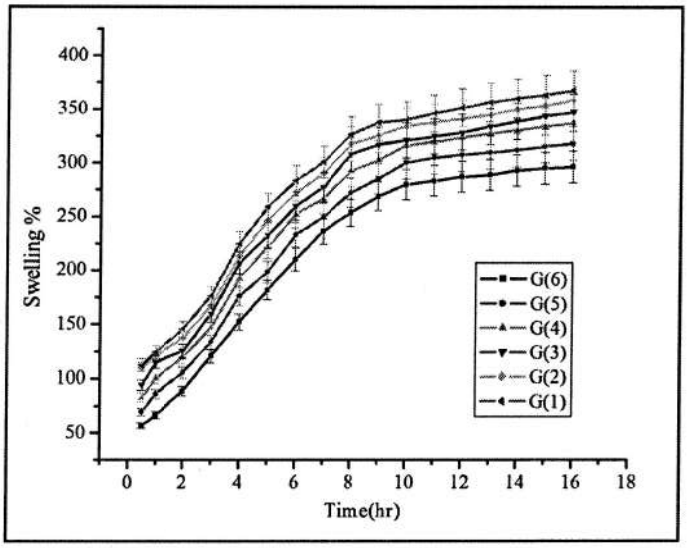

Fig.13 Effect of OMMT nanoclay on the swelling properties of the nanocomposite hydrogel.

Presence of crosslinker is an important pre-requisite for formation of ideal three-dimensional networks of hydrogels. It was observed that the swelling capacity of the nanocomposite hydrogels decreased with the increase in crosslinker amount. According to Flory's theory,[4] the excessive crosslinking may cause the generation of more crosslinking points during radical polymerization and the increase of crosslinking density of polymer network, and so the water absorption of the hydrogel was decreased with increasing the concentration of crosslinker.

Swelling behaviour is observed to be varied with the network parameters such as the polymer volume fraction in swollen state $\upsilon_{2,s}$, molecular weight of the polymer chain between two neighboring crosslinking points ($\overline{M_c}$) and the correlation length or mesh size (ξ). Table 2 represents the calculated values of these parameters found in case of the prepared nanocomposite hydrogel. It can be seen that mesh size (ξ) decreases with increasing polymer volume fraction and accordingly swelling % decreases. Also, gradual increase of crosslinker leads to a compact network which results low value of ξ and $\overline{M_c}$, indicating that the network meshes were less open with the higher amount of crosslinker. For that, there will be a fall in the swelling percentage of the hydrogels.

1.4.5 Bending behaviour under an electric field

The exact mechanism of bending of ionic polymer films has not been fully understood, it is generally thought that the deformation of a hydrogel film under an electric field is due to the voltage-induced motion of ions. When a strip of PVA-g-PAA/OMMT nanocomposite hydrogel, in an aqueous solution of NaCl, was subjected to an electric filed, the hydrogel showed significant and quick bending towards the cathode. Again, if the electric stimulus was removed, it returned to its original position. The same behaviour was not observed in pure water. This implies that the bending of the hydrogels was induced by electro-chemical reactions. The bending behaviors of the hydrogels under different applied voltages are shown in Fig. 13. It can be seen that both the bending speed and the maximum bending angle of hydrogel increased with the increasing of applied voltage, indicating that bending is induced by an electric current.[9] It is thought that the counterions (cations) of the polyion, which is an ionic group in the polymer network, moves toward the negative electrode. The polyion (anion) remains immobile. The free ions in the surrounding solution move towards their counter electrode and come in contact with the gel. Therefore, the osmotic pressure of the gel polymer network near the positive electrode increases and becomes larger than that of the negative electrode side. Consequently, the osmotic pressure difference occurs within the gel and is the driving force that controls bending toward the negative electrode. The effect of voltage on bending phenomenon has been investigated in the range 3.0 to 12.0 V. No bending was observed below 3.0V; so, lower critical voltage (LCV) found in this case is 3.0volt.

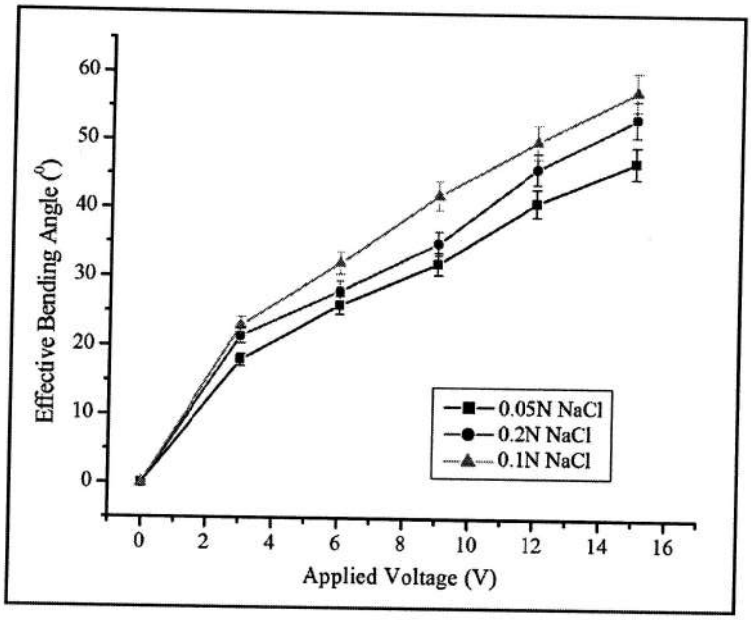

Fig.13 Effect of the aqueous NaCl solution concentration on the equilibrium bending angle (EBA) at different applied voltages.

The influence of the medium ionic concentration on the bending behavior of the nanocomposite hydrogels were determined by varying the concentrations of aqueous NaCl solution from 0.05N to 0.2 N respectively. It was observed that the bending degree increased when the concentration of aqueous NaCl solution was increased from 0.05N to 0.1N, but again decreased when concentration of NaCl exceeds 0.1N. May be, an increase in the electrolyte concentration in a solution induces an increase of the free ions moving from the surrounding solution toward their counter electrode or into the hydrogel. So, the bending degree of the hydrogel increased when concentration of NaCl was increased from 0.05N to 0.1N. But after an optimum electrolyte concentration, the shielding effect of the polyions by the ions in the electrolytic solute occurs which leads to a reduction in the electrostatic repulsion of the polyions and a decrease in the degree of bending. A similar result was reported in our previous study of bending behaviors of composite hydrogels composed of poly(acrylic acid-co acrylamide) and polyaniline.[11]

Conclusion

In this study, nanocomposite hydrogels of PVA, partially neutralized acrylic acid and layered organically modified OMMT clay were prepared by free radical graft polymerization reaction. The grafting reaction of acrylic acid on PVA was confirmed by FTIR. X-ray diffraction analysis showed that the nanocomposite forms a partially exfoliated or intercalated structure. Also, SEM studies demonstrated a finer dispersion of the clay particles in nanocomposite as compared to the composite. Swelling percentage of the nanocomposite hydrogel was found to be decreased with increasing crosslinker amount. Since, crosslinking density of composite increased with the increase of OMMT content, so there was decrease in water absorbency. The bending behaviour

of the prepared hydrogels under applied electric field was also investigated with respect to the applied voltage and ionic strength of the polyelectrolyte solution. The nanocomposite hydrogels showed significant and quick bending towards the cathode. This behavior suggests the possibility of application as an artificial muscle and also other uses like sensors, switches and electric current modulated drug delivery systems etc.

(c) Electric Field Assisted Drug Release from pH and electro-responsive Gelatin-*g*-poly(acrylic acid)/MWCNTs nanocomposite hydrogels:

1. Experimental

1.1 Materials

Acrylic acid monomer (Aldrich) was distilled under reduced pressure prior to use. Gelatin A (300 Bloom), ammonium persulfate (initiator), methylene bis-acrylamide (MBA) as a crosslinking agent and N, N, N,' N'- tetramethylethylene diamine were supplied by Aldrich (A.R. grade). Multiwall carbon nanotubes (MWCNTs) were supplied from Shenzhen Nanotech Port Co., Ltd., China. Nitric acid, sodium hydroxide and ethanol (A. R grade) were purchased from Merck, Mumbai. Vitamin B_{12} ($C_{63}H_{88}CoN_{14}O_{14}P$) was purchased from Merck, Mumbai (M.W= 1355.4 g/mol).

1.2 Acid treatment of MWCNT

Functionalization of CNTs with different chemical groups is generally used to enhance their dispersibility in water and the mostly used technique for this purpose is the oxidization with strong oxidants to generate carboxyl group on the surface of CNTs. In this case, the carboxylic acid functionalized MWCNTs were prepared according to the earlier described method.[10, 11] 60 mg of MWCNTs were added to a round-bottom flask containing 50ml of 60% HNO_3 aqueous solution. The mixture was refluxed for 6 hrs and then cooled to room temperature. The mixture was diluted with 500 ml of deionized water and then collected by low speed centrifugation. The obtained product was washed with deionized water until the pH of the filtrate reached 7 and was dried under vacuum for 24 h at 80°C.

1.3 Fabrication of Gelatin-*g*-polyacrylic acid/MWCNT-COOH nanocomposite hydrogel

Gelatin-*g*-polyacrylic acid /MWCNT-COOH nanocomposite hydrogels were prepared by free radical polymerization in distilled water. 2 g of gelatin was dissolved in 30 ml of distilled water at 60°C and 1.5 ml of partially neutralized (60%) acrylic acid monomer was added to this solution. Also, MWCNT-COOH (0.1-0.6 wt%) was added to gelatin-acrylic acid mixture and

dispersed under the ultrasonic vibration for 30 min. Subsequently, methylene bis-acrylamide (0.05-0.25 wt%), ammonium persulfate (1.0 wt%) and TEMED (0.05ml) were added to the mixture under continuous stirring. Nitrogen was used to remove dissolved oxygen from the reactive solution. The reactive solution was first prepolymerizd at 60°C for 1h under stirring, and then poured into a petri dish quickly. The post polymerization was carried out at 70°C for 3 h. When the reaction was completed, the nanocomposite hydrogel was cut into (3×3 cm) blocks and immersed in repeatedly changed deionized water for 72 h to remove the residual monomers. Table 1 and 2 outline the feed compositions of subsequently prepared hydrogels. Also, a schematic diagram for the preparation of nanocomposite hydrogel is shown in Scheme 1.

Table 1 Recipe in the preparation of Gelatin-g-PAA/MWCNT-COOH nanocomposite hydrogel

Recipe	GA	GA-1	GA-2	GA-3	GA-4	GA-5	GA-6
Gelatin(g)	2	2	2	2	2	2	2
Acrylic acid (g)	7.2	7.2	7.2	7.2	7.2	7.2	7.2
Multiwall carbon naonotubes (wt%)	0	0.1	0.2	0.3	0.4	0.5	0.6

with different crosslinker (MBA) content:

* Tetramethylethylene diamine (ml) = 0.05ml, MWCNT-COOH (wt%) = 0.4 and ammonium persulphate (wt%) = 0.1

Table 2 Recipe in the preparation of Gelatin-g-PAAc/MWCNT-COOH nanocomposite hydrogel with different MWCNT-COOH content:

* Tetramethylethylene diamine (ml) = 0.05ml, methylene bis-acrylamide (wt%) = 0.15 and ammonium persulphate (wt%) = 0.1

Recipe	GM-1	GM-2	GM-3	GM-4	GM-5
Gelatin(g)	2	2	2	2	2
Acrylic acid (g)	7.2	7.2	7.2	7.2	7.2
Methylene bis-acrylamide (wt%)	0.05	0.1	0.15	0.2	0.25
Gel fraction (%)	54	62	74	82	91
Ionic Conductivity (S/cm $\times 10^{-2}$)	2.50	1.94	1.72	1.58	1.37

Ionic Conductivity (S/cm $\times 10^{-2}$)	0.92	1.65	2.2	2.85	3.41	3.92	4.52

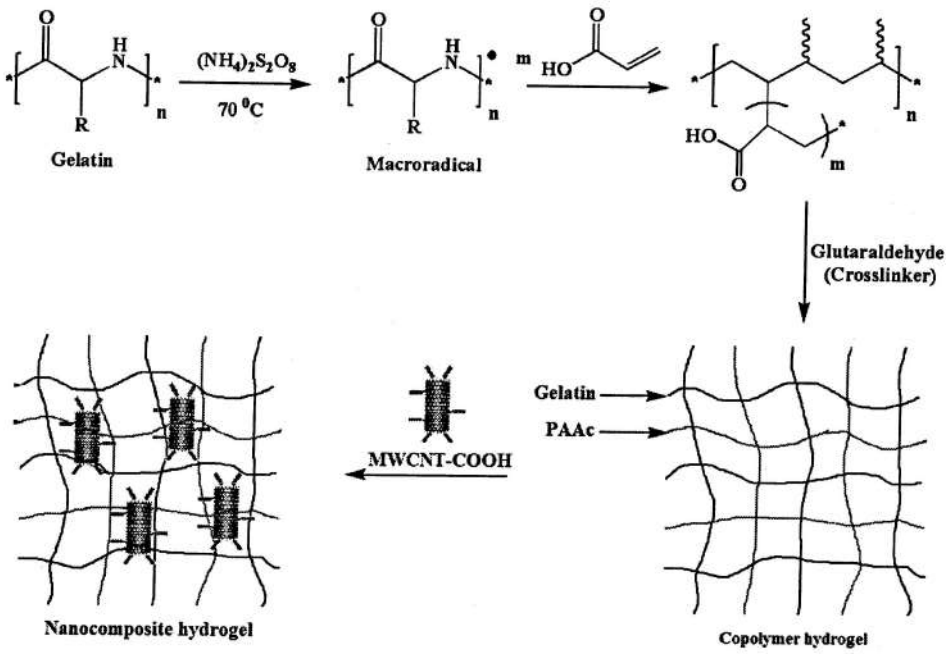

Scheme 1. Schematic representation for the formation of Gelatin-*g*-PAAc/MWCNT-COOH nanocomposite hydrogel.

1.4 Characterizations of the nanocomposite hydrogel

Fourier transform infrared spectroscopy (FTIR) was used to record FTIR spectra by Impact 410, Nicolet, USA, using KBr pellets. Powder X-Ray diffraction (XRD) data were collected on a Rigaku Miniflex X-ray diffractometer (Tokyo, Japan) with Cu Kα radiation (λ=0.15418 nm) at 30 kV and 15 mA with a scanning rate of 0.05^0s^{-1} in a 2θ ranges from 20^0 to 80^0. The surface morphology of the composites was observed using a scanning electron microscope (SEM) (Model- JSM-6390LV, JEOL, Japan). The surface of the sample was coated with platinum before SEM analysis. Further morphological analysis was done by Transmission electron microscope (JEM 2100) with an acceleration voltage of 200 kv. IV characteristics were studied by Keitheley 2400 source meter at the room temperature in the frequency range 102-106 Hz. The voltage was applied to measure the current passing through the sample.

1.5 Swelling properties

To measure the degree of swelling the hydrogels, dried samples were placed in buffer media of different pH values at room temperature until the hydrated gels reached a stable weight. The swelling behavior under an applied electric field was determined by applying different electric

potentials to the nanocomposite hydrogel in distilled water. The water absorbed on the surface of the hydrogels was removed using filter paper and the weight noted.

$$\text{Swelling } \% = W_s\text{-}W_{dry}/W_{dry} \times 100 \qquad (1)$$

Where, W_s is the weight of the hydrogel in swollen state and W_{dry} is that of the hydrogel in dry state.

1.6 Blood compatibility by hemolytic activity assay

The hemolytic test was performed following the protocol of Das Purkayastha, M. et al, with slight modification.[3] Briefly, fresh goat blood from a slaughterhouse was collected in a centrifuge tube containing anticoagulant, trisodium citrate (3.2%), and was centrifuged at 2500 rpm for 10 min. The supernatant was discarded, and only the erythrocytes were collected. The erythrocytes were further washed three times with PBS (pH 7.4). A 5% (v/v) suspension of erythrocytes in PBS was prepared; 0.95 ml of this erythrocyte solution was placed in a 1.5 ml centrifuge tube, and 0.05 ml of sample (0.5mg dissolved in 1 ml of 0.5% DMSO) was added to it. The tubes were then incubated for 1 h at 37°C. Triton X-100 (0.2 %) and PBS were taken as the positive and negative controls, respectively, for comparison. After incubation, the tubes were subjected to centrifugation at 2500 rpm for 10 min. Then, 0.2 ml of the supernatant was added to 96-well plate, and finally absorbance was taken at 570 nm in a UV–visible spectrophotometer (Shimadzu UV-2550 UV–vis spectrophotometer).

$$\text{Hemolysis } \% = [(\text{Sample O.D} - \text{Negative control O.D})/ (\text{Positive control O.D} - \text{Negative control O.D}] \text{ X } 100 \qquad (2)$$

1.7 Loading of vitamin B_{12}

The method of soaking or equilibration was employed for vitamin B_{12} loading. In this method, the amount of buffer necessary for complete swelling of the nanocomposite hydrogel was determined.[12] Dry hydrogel was placed in the drug solution at a concentration of 0.125 wt%, prepared in the buffer solution of pH 7.0 and left until all the drug solution was sucked up. Then the completely swollen hydrogel loaded with the vitamin B_{12} was placed in an oven at 30°C for drying overnight.

1.8 Drug release experiment under electric field

To investigate the release behavior of vitamin B_{12} under electric stimulus, drug loaded hydrogels were placed in the middle of two carbon electrodes in a desired release medium as shown in the

Fig. 14. Then, the amount of drug released into the respective medium was monitored by varying factors such as ionic strength of the release medium and the MWCNT-COOH content in the nanocomposite hydrogel. The pulsatile release of vitamin B_{12} under the applied electric field was also determined by applying pulses of electric current at 5 V, 30 min on and 30 min off. At scheduled time intervals, 5 ml solution was withdrawn and assayed spectrophotometrically by using a UV-Visible spectrophotometer (UV-2001Hitachi, Japan) for the determination of the cumulative amount of drug release from the absorbance at 362nm. To maintain a constant volume, 5 ml of the same solution was returned to the container. The amount of vitamin B_{12} released from the nanocomposite hydrogel was calculated from a calculated from a previously calibrated standard curve.[13]

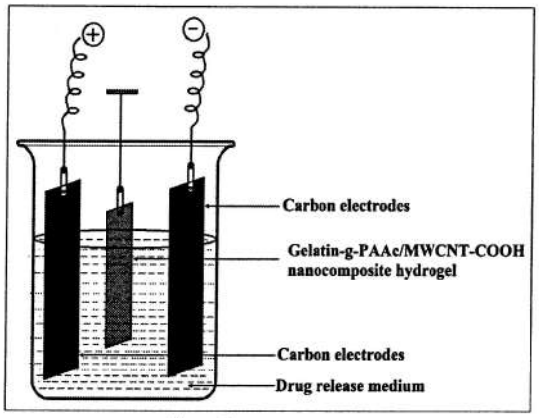

Figure 1

Fig. 14 Apparatus for electro-responsive drug delivery.

2. Results and Discussions

2.1 FTIR spectrum analysis

FTIR spectra of pristine MWCNT, acid functionalized MWCNT, Gelatin-*g*-PAAc/MWCNT-COOH nanocomposite hydrogels and Gelatin-g-PAAc copolymer are shown in the Fig. 15 (a, b, c, d). The characteristic bands due to generated polar functional groups on the MWCNT are observed in the FTIR spectrum of the MWCNTs after chemical oxidation in HNO_3 acid. The FTIR spectrum of MWCNT–COOH shows absorption peak at 2910 cm^{-1} corresponding to the C-H symmetric stretching vibration. Also, the appearance of peak at 1531 cm^{-1} confirms the existence of carbon double bonding (C=C), which again reveals the integrity of hexagonal structure on the pristine MWCNT.[6] Appearance of peak at 1725 cm^{-1} assigns carbonyl (C=O) stretching vibration of carboxyl groups which is not present in pristine MWCNTs. It confirms the carboxylation on the surfaces of functionalized MWCNTs (Fig. 15b).

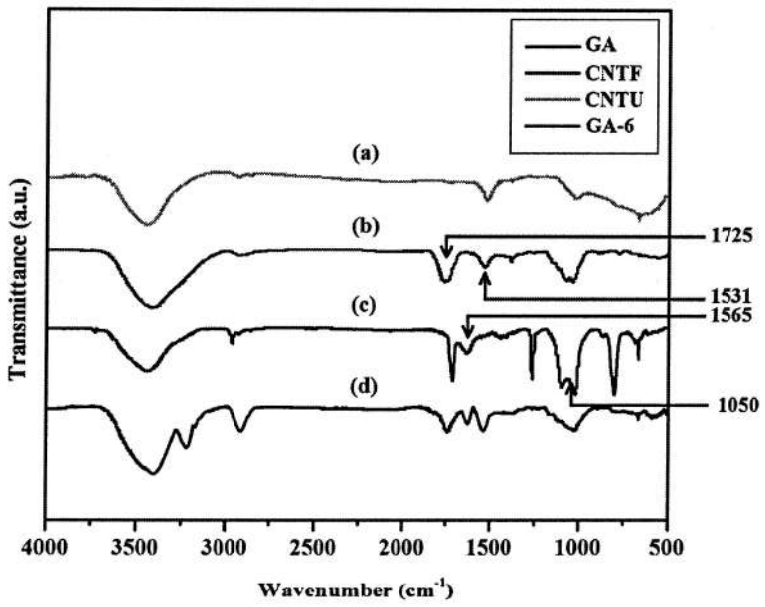

Fig. 15 FTIR spectra of (a) MWCNT-pristine, (b) MWCNT-COOH, (c) Gelatin-*g*-PAAc/MWCNT-COOH nanocomposite hydrogels and (d) Gelatin-*g*-PAAc hydrogel.

FTIR spectrum of Gelatin-g-PAAc shows absorption peaks at 3391 cm^{-1} and 2950 cm^{-1} which are attributed to the N-H stretching vibration and C-H stretching vibration in $-CH_3$ group. The peaks at 1630 cm^{-1} and 1520 cm^{-1} are due to the amide I (C=O stretching vibration) and amide II (-NH bending vibration) respectively. The absorption peak at 1126 cm^{-1} is due to the C-N stretching vibration of amide III. Also, the characteristic peaks at 3450 cm^{-1}, 1735 cm^{-1} and 613 cm^{-1} are due to the -OH stretching vibration of PAAc, C=O stretching vibration and the -OH out of plane vibration of the carboxylic groups of PAAc, which confirms the grafting reaction. Fig. 15c represents the FTIR spectrum of Gelatin-*g*-PAAc/MWCNT-COOH nanocomposite hydrogel which shows characteristics peaks of MWCNT–COOH at 1565 cm^{-1} which is ascribed to the C=C bonding that forms the framework of the carbon nanotube sidewall. The peak at 1050 cm^{-1} indicates the presence of –COOH groups of carboxylated MWCNT and the peaks present in 500-1000 cm^{-1} range indicates the presence of hexagonal carbon atom. Presence of all these characteristics peaks indicates the incorporation of MWCNT–COOH into the Gelatin-*g*-PAAc hydrogel matrix.

2.2 XRD analysis

The diffraction peaks with 2θ values of 25.54° and 45.70° are found for pristine MWCNTs and the diffraction peaks at 2θ of 26.08° and 43.08° are attributed to the graphite structure (002) and (100) planes of the MWCNT-COOH as shown in the Fig. 16a and b. The shifting of characteristic peak position in the XRD pattern of MWCNT-COOH shows the perfect modification of pristine MWCNTs. There is no drastic change in the position of characteristic

peaks of pristine MWCNTs and MWCNT-COOH was observed, which suggest that MWCNTs are well retained their original structure even after functionalization.[14]

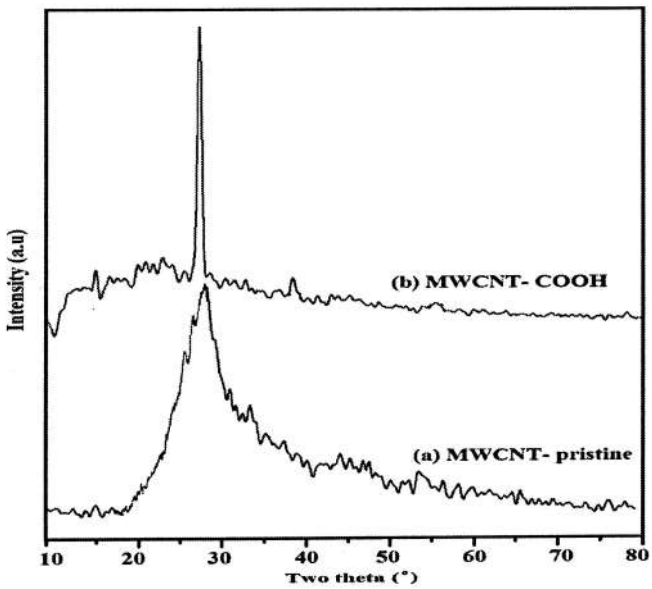

Fig. 16 XRD patterns of (a) MWCNT-pristine and (b) MWCNT-COOH.

Fig. 17a and b depicts the XRD patterns of Gelatin-*g*-PAAc copolymer hydrogel and Gelatin-*g*-PAAc/MWCNT-COOH nanocomposite hydrogels respectively. The XRD pattern of Gelatin-g-PAAc doesn't possess any characteristics peaks, but some minor peaks were observed around 21° and 22°, which could be attributed to minor crystallites of grafted polyacrylic acid chains. On the other hand, the XRD pattern of Gelatin-*g*-PAAc/MWCNT-COOH shows the characteristics peaks of MWCNT-COOH with low intensity which confirms the incorporation of acid functionalized multiwall carbon nanotubes into the Gelatin-*g*-PAAc hydrogels.

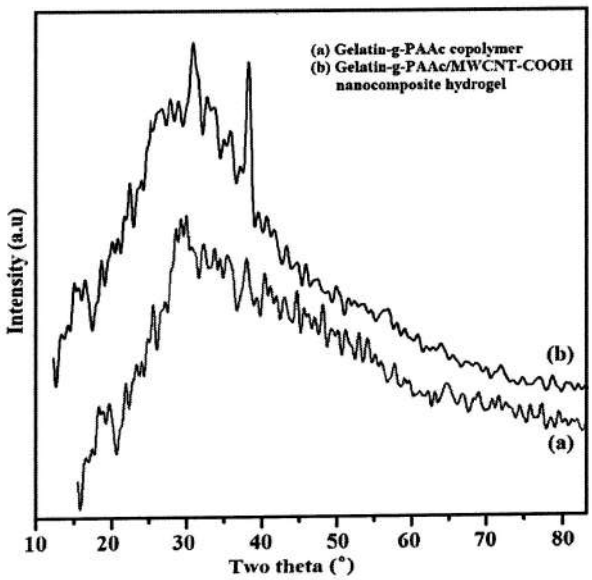

Fig. 17 XRD patterns of (a) Gelatin-*g*-PAAc hydrogel and (b) Gelatin-*g*-PAAc/MWCNT-COOH nanocomposite hydrogels.

2.3 Morphological analysis

The morphological images of the copolymer hydrogel and MWCNT-COOH incorporated hydrogels were studied by SEM and are shown in Fig. 18a and b. SEM micrographs indicate the change in the surface morphology of the prepared hydrogels after the incorporation of MWCNT-COOH. A rough surface morphology is observed and some pores are can be observed in the micrograph of Gelatin-g-PAAc hydrogel. But, comparatively a smooth surface was observed after the impregnation of MWCNT-COOH into the hydrogel. This observation implies that MWCNT-COOH is uniformly dispersed within the hydrogel. Also, scanning electron microscopy was used to investigate possible MWCNTs fragmentation occurred during treatment. SEM images of pristine MWCNT and MWCNT-COOH are shown in the Fig. 18c and d. From both the micrographs, a significant difference was observed. A sharp surface was observed for the functionalized MWCNT, which was apparently smooth in case of pristine MWCNT. Also, the transparency of nanotubes has also been decreased after the functionalization as compared to the pristine MWCNTs which possibly related the introducing of functional groups.[15, 16]

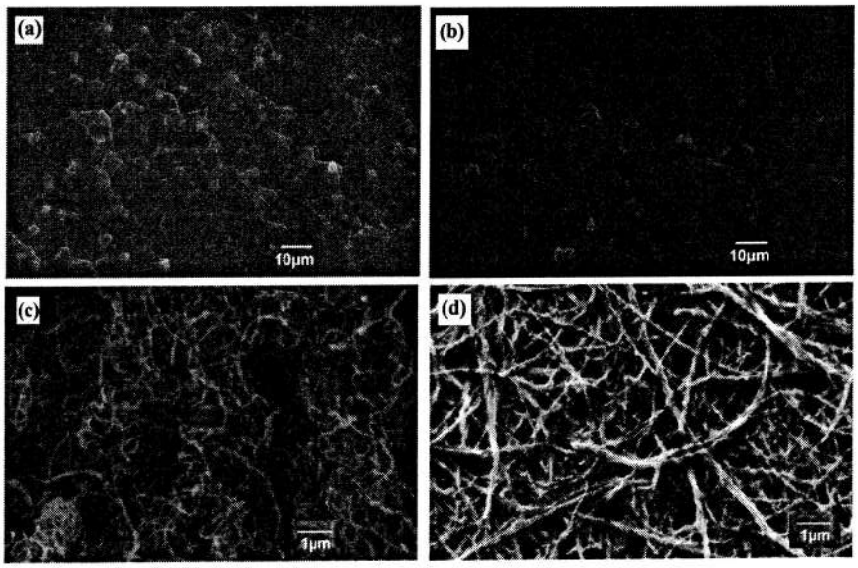

Fig. 18 SEM images of (a) Gelatin-*g*-PAAc hydrogel, (b) Gelatin-*g*-PAAc/MWCNT-COOH nanocomposite hydrogels, (c) MWCNT-pristine and (d) MWCNT-COOH.

Further functionalized MWCNTs morphology characterization was conducted using TEM analysis and Fig. 18 represents the TEM micrographs of MWCNT-COOH and Gelatin-*g*-PAAc/MWCNT-COOH nanocomposite hydrogel respectively. No structural damage occurred after acid functionalization of MWCNTs. The MWCNTs retained their original morphology even after the acid treatment. Also, the stable and uniform dispersion of the MWCNT-COOH within the Gelatin-*g*-PAAc matrix is evident from the TEM study. The TEM image (Fig. 19a) shows that the MWCNT-COOH has an average external diameter of 20-25 nm. A representative TEM image shows the anchoring of a gelatin-*g*-PAAc layer onto a MWCNT-COOH with a diameter of 30-35 nm (Fig. 19b). This increase in the diameter in the nanocomposite hydrogel indicates the presence of a layer of Gelatin-*g*-PAAc molecules on the surface of the MWCNT-COOH.

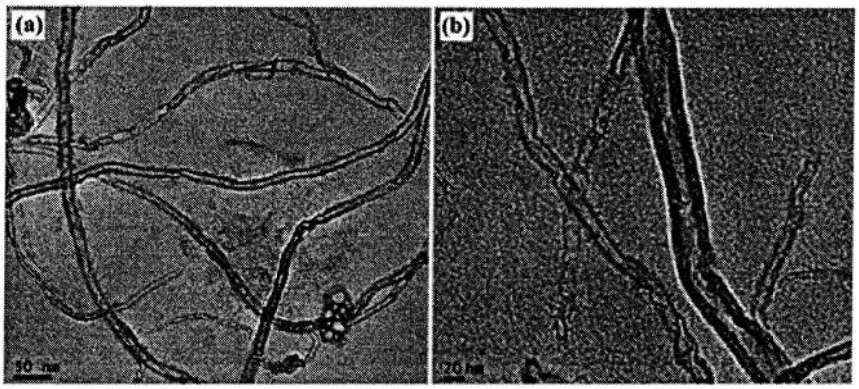

Fig. 19 TEM images of (a) MWCNT-COOH and (b) Gelatin-*g*-PAAc/MWCNT-COOH nanocomposite hydrogels.

2.4 Swelling study

2.4.1 Effect of pH

The hydrogels have shown tremendous promise in different biomaterial applications because of their unique water holding capacity. Hence, swelling behavior of a particular hydrogel material should be investigated in order to confirm its utility in different biomedical areas. Fig. 20 represents the swelling behavior of the nanocomposite hydrogel (GM-3, 0.15 wt% methylene bis-acrylamide) in acidic (pH=4) and basic (pH=7.4) medium. The swelling behavior was found to be increased with an increase in pH from 4 to 7.4. The gelatin structure is ionizable because the basic dissociation constant (pK_b) of the NH_3^+ is about 6.5 and the acid dissociation constant (pK_a) of the COOH is about 4.7 in gelatin.[17] So, this improved swelling behavior is due to the presence of the hydrophillic functional groups (mainly COO^-) in the gelatin structure. Moreover, at higher pH, ionization of the carboxylic acid groups occurs, resulting in electrostatic repulsion between the carboxylate ($-COO^-$) groups as well as expansion of the space network thereby increasing the swelling percentage.[18]

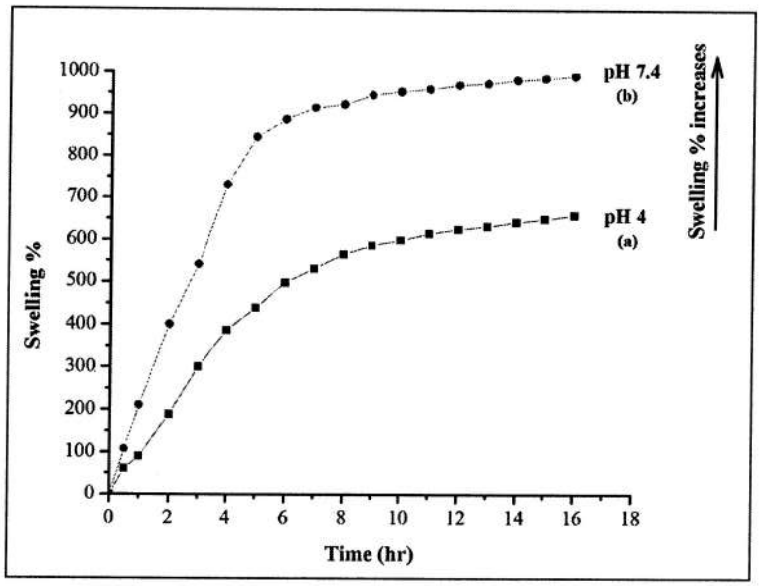

Fig. 20 Influence of pH of the medium on the swelling behaviour of the nanocomposite hydrogel (GM-3, 0.15 wt% methylene bis-acrylamide): (a) pH = 4 and (b) pH = 7.4.

2.4.2 Effect of MWCNT-COOH

Fig. 21a depicts the effect of MWCNT-COOH content on the swelling behavior of Gelatin-*g*-PAAc hydrogels. It was observed that the extent of swelling was decreased with an increase in the concentration of MWCNT-COOH. It may be mainly due to the hydrophobic nature of the MWCNT-COOH. The result is consistent with other reports in the literature.[19] Moreover, functionalized MWCNT in Gelatin-*g*-PAAc may acts as like some crosslinking sites which make the diffusion of water into the hydrogel more difficult. So, interaction between MWCNT-COOH and hydrogels contributed to lower the swelling percentage of the nanocomposite hydrogels than for the native gel.

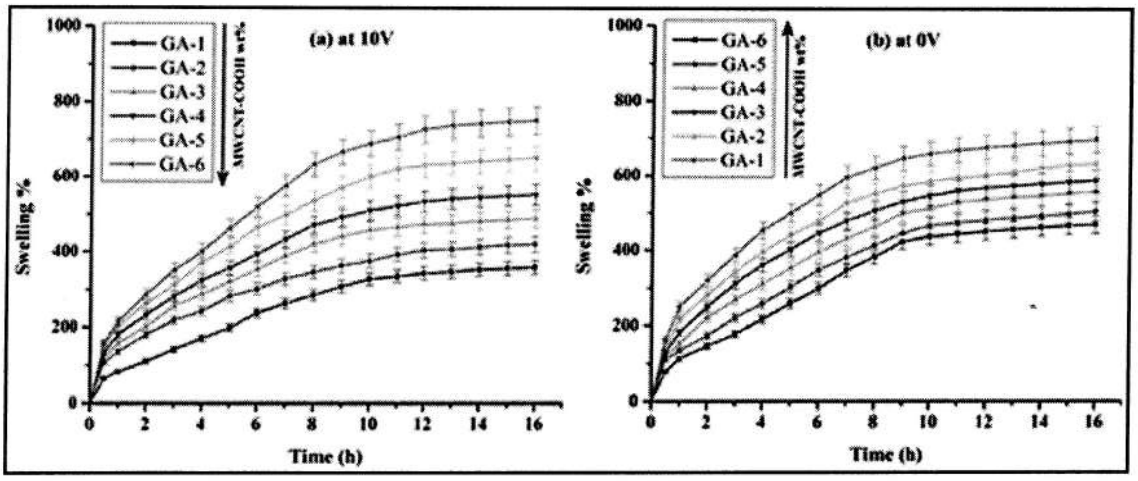

Fig. 21 Effect of MWCNT-COOH content on the swelling behavior of Gelatin-*g*-PAAc hydrogels: (a) at 0V and (b) at 10V.

2.4.3 Effect of applied electric field

The response of an electro-responsive hydrogel in presence of an external electric field depends on the shape and position of the gel between the electrodes.[20] When the gel is placed at a fixed position away from the electrodes, as in our experiment, the swelling behaviour is observed. So, the swelling behavior of the nanocomposite hydrogel with various MWCNT-COOH content were measured as a function of time in distilled water under the applied electric potential of 10V. The swelling percentage of Gelatin-*g*-PAAc/MWCNT-COOH gradually increased with increasing MWCNT-COOH content (Fig. 21b). MWCNT-COOH provides the efficient pathway of electric field. Therefore, MWCNTs could contribute to the increase in swelling percentage of the nanocomposites by increasing the extent of ionization of the functional groups in the nanocomposite hydrogel under electric voltage applied. This behavior is completely opposite to the swelling character under normal condition where swelling percentage decreases with increase in MWCNT-COOH content.

2.5 Blood compatibility studies

Numerous efforts have been given to design novel biomaterials with superior blood compatibility by various research groups. Hemocompatibility is a prime requirement for biomedical applications such as drug delivery, tissue engineering etc. intended for direct or indirect blood exposure. Fig. 22 represents the data obtained from hemolysis test. The hemolysis test was performed for the nanocomposite hydrogels with 0.1 and 0.6 wt% of MWCNT-COOH content with different concentrations. For all samples while contact with blood, showed a mean hemolysis value less than 0.5 %. The sample with 0.6 wt% of MWCNT-COOH content showed less hemolytic activity than the sample with 0.1 wt% MWCNT-COOH, as the presence of carboxyl group on MWCNT improved its biocompatibility. The overall test showed very low hemolysis activity and the data obtained are at the permissible limit as shown in the Fig. 22a. Photographs showing precipitated RBCs at the end of the hemolysis experiment are also given in Fig. 22b.

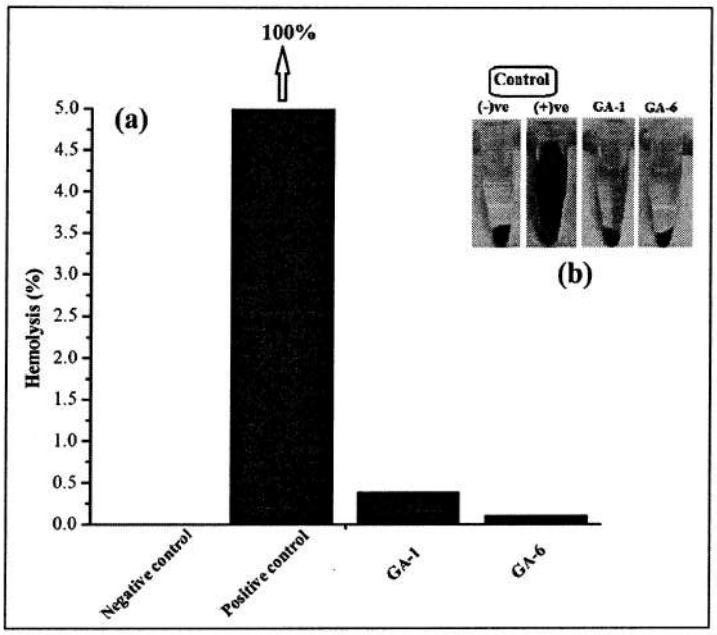

Fig. 22 Hemolysis results: (a) Hemolysis percentage of the nanocomposite hydrogels with 0.6 wt% (GA-6) and 0.1 wt% (GA-6) MWCNT-COOH content, (b) Photographs of RBCs treated with different samples (GA-6 and GA-1).

2.6 Electro-responsive release behavior of vitamin B_{12} from Gelatin-*g*-polyacrylic acid/MWCNT-COOH nanocomposite hydrogels:

2.6.1 Effect of applied voltage

The effect of applied electric potential on release behavior of vitamin B_{12} from Gelatin-*g*-PAAc/MWCNT-COOH nanocomposite hydrogel is shown in Fig. 23a and b. It can be observed that the drug release rate was much higher under the influence of an electrical stimulus than without electric stimulus. A systematic increase in the drug release rate was observed when the applied voltage was increased from 5V to 10V. According to Sawahata et al. drug transport occurs only if the applied electrical current is sufficiently high to induce dimensional changes in the hydrogel. Under higher applied voltage, the ionizable groups are more ionized which results in improved swelling behavior of the nanocomposite hydrogel. The improved swelling will enhance the release of drug from the nanocomposite hydrogel through diffusion.[21,22]

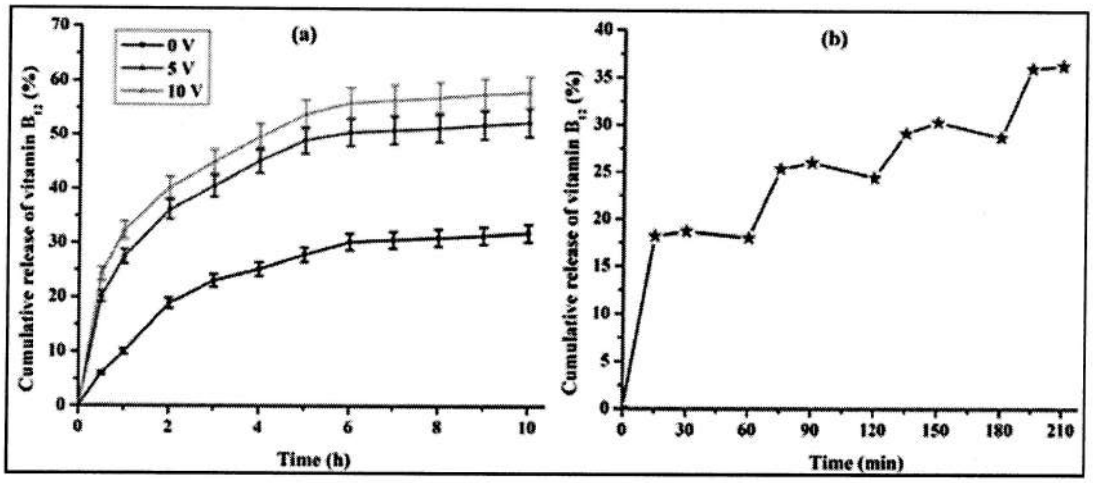

Fig. 23 Drug release behavior of Gelatin-*g*-PAAc/MWCNT-COOH nanocomposite hydrogels- (a) At different electric voltage applied: 0 V, 5V and 10 V, (b) Drug release behavior as a function of applied voltage of 0V and 5V, which was altered at 30-min time intervals.

Moreover, the rapid release behaviors of vitamin B_{12} were observed when an electric stimulus was at "on" state (Fig. 23b), whereas they showed a relatively slow release rate during the "off" state while applied electric potential was maintained at 0 and 5V alternately. The plausible reason for this switching pattern of the release of drug molecules is due to the electrically induced changes in osmotic pressure within the gel and local pH gradient attributed to water electrolysis.[23] This could also affect the swelling behaviour of the nanocomposite hydrogel under electric field as well as release of drug from the Gelatin-*g*-PAAc/MWCNT-COOH nanocomposite hydrogel. In 'off' stage (when no electric field), normal diffusion controlled release of drug is taking place which is quite slow.

2.6.2 Effect of MWCNT-COOH content

The release of vitamin B_{12} was found to be profoundly dependent on the MWCNT-COOH content of the nanocomposite hydrogels. It can be seen from Fig. 24a, that the drug release rate was decreased as the content of MWCNT-COOH increased when no electric field was applied. On the other hand, a reverse release behavior was observed when an electric potential of 10V was applied to the nanocomposite hydrogels. The release of vitamin B_{12} was found to be increased with increase in MWCNT-COOH content, as predicted from the swelling behavior of nanocomposites in presence of an electric field displayed in Fig. 24b.

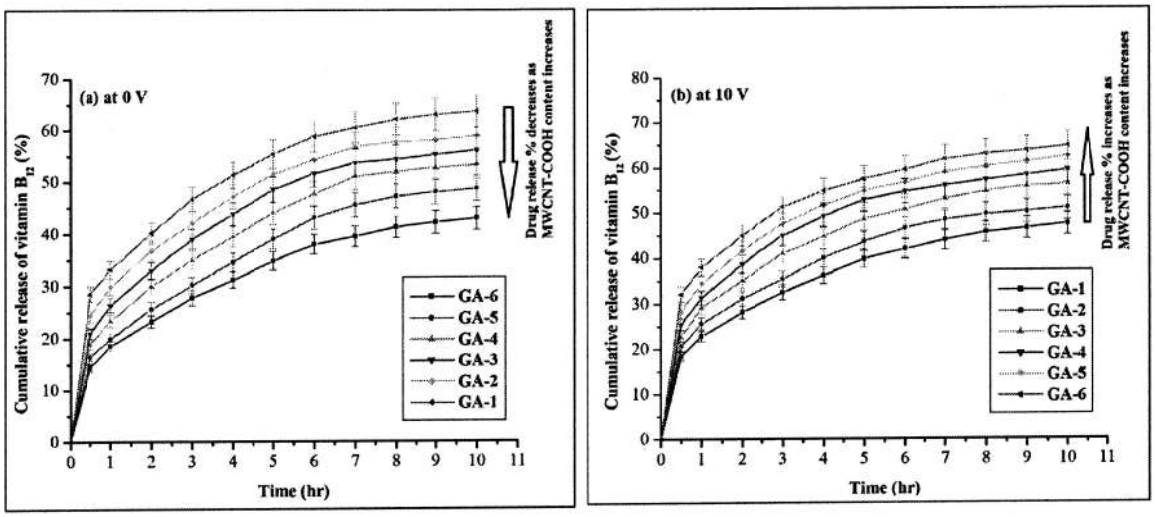

Fig. 24 Drug release behavior of various Gelatin-*g*-PAAc/MWCNT-COOH nanocomposite hydrogels at different electric voltage applied: (a) 0 V and (b) 10 V.

3. Conclusion

In the present study, nanocomposite hydrogels based on gelatin, partially neutralized acrylic acid and acid functionalized multiwall carbon nanotubes (MWCNT-COOH) have been developed. The shifting of characteristic peak position in the XRD pattern of MWCNT-COOH shows the perfect modification of pristine MWCNTs. The characteristics peaks of MWCNT-COOH in the XRD pattern of Gelatin-*g*-PAAc/MWCNT-COOH confirm the incorporation of acid functionalized multiwall carbon nanotubes into the nanocomposite hydrogels. Also, TEM studies confirm the uniform dispersion of MWCNT-COOH within the nanocomposite hydrogel. From the swelling behaviour, it was observed that the swelling percentage was more in basic medium (pH 7.4) than in acidic medium (pH 4) due to the more ionization of the carboxylic acid groups. The MWCNT-COOH content also affects the swelling properties of the hydrogel to a greater extent. The swelling percentage was found to be decreased with an increase in MWCNT-COOH content, when no electric field was applied; but reversed swelling behavior was observed when an external electric field (10V) was applied. *In vitro* experiments of percentage hemolysis reveal that the prepared nanocomposite hydrogels possess proficient blood compatibility suitable for biomedical applications. The electro-responsive release behavior of vitamin B_{12} exhibited a considerable dependence on applied voltage and MWCNT-COOH content of the nanocomposite hydrogels. So, the results obtained in this work lead us to the conclusion that Gelatin-*g*-PAAc/MWCNT-COOH nanocomposite hydrogels can be a promising platform for the development of electro-responsive drug delivery systems.

List of paper published:

1. Biocompatible carboxymethylcellulose-g-poly(acrylic acid)/OMMT nanocomposite hydrogel for in vitro release of vitamin B12, M. Boruah, Pr. Gogoi, A. K. Manhar, Mo. Khannam, M. Mandalb and S. K. Dolui, *RSC Adv.*, **2014**,4, 43865-43873.

2. Electrical actuation of electroresponsive hydrogels based on poly(acrylamide-co-acrylic acid)/graphite suitable for biomedical applications, M. Boruah, P. Phukon, B.J. Saikia and S.K. Dolui, *Polym Compos*, **2014**,35,27–36.

3. Synthesis and Characterization of pH Responsive Conductive Composites of Poly(acrylic acid-co-acrylamide) Impregnated with Polyaniline by Interfacial Polymerization, M. Boruah, A. Kalita, B. Pokhrel, S. K. Dolui, and Ratan Boruah, *Adv. Polym. Technol,* .**2013**, 13, E520–E530.

4. Synthesis of pH- and solvent-responsive smart core crosslinked star polymer by atom transfer radical polymerization, B. J. Saiki, P. Gogoi, S. Sharmah and S. K. Dolui, *Polym. Int.*, **2015**, 64, 437–445.

5. Mn2+ anchored CdS polymer nanocomposites: An efficient alternative for Mn2+ doped CdS nanoparticles, B. J. Saikia, B. C. Nath, C. Boraha, S. K. Dolui, *Journal of Lumin.* **2015**,168, 178–185.

References:

1. A. K. Bajpai, J. Bajpai, and C.N. Soni, *eXPRESS Polym. Lett.* **2**, 26 (2008).
2. S. Sun and A. F. T. Mak, *J. Polym. Sci. Part B Polym. Phy.* **39**, 236 (2001).
3. S. J. Kim, S. G. Yoon, Y. H. Lee, and S. I. Kim, *Polym. Int.* **53**, 1456 (2004).
4. P. J. Flory, *Principles of Polymer Chemistry,* 2nd ed. New York: Cornell University Press, Ithaca (1992).
5. A. Samakande, P. C. Hartmann, V. Cloete, and R. D. Sanderson, *Polymer,* **48,** 1490 (2007).
6. Y. Zheng and A. Wang. *Polym. Compos.,* DOI 10.1002/pc. 20670(2009).
7. N. A. Peppas and A. G. Mikos, *Hydrogels Med. Pharm.,* **3,** 1 (1986).
8. X. Jin and L. Y. Hsieh, *Polymer,* **46,** 5149 (2005).
9. M. Boruah, P. Phukon, B. J. Saikia, and S. K. Dolui, *Polym.Compos.,* DOI 10.1002/pc.22630 (2013).

10. J. Chen, M. A. Hamon, H. Hu, Y. Chen, A. M. Rao, P. C. Eklund and R. C. Haddon, *Science,* 1998, **282,** 95-98.

11. K. A. Worsley, I. Kalinina, E. Bekyarova and R. C. Haddon, *J. Am. Chem. Soc.,* 2009, **131,** 18153–18158.

12. M. D. Purkayastha, S. Das, A. K. Manhar, D. Deka, M. Mandal and C. L Mahanta, *J. Agric. Food Chem.,* 2013, **61,** 10746-10756.

13. S. K. Bajpai, M. Bajpai and L. Sharma, *Iran. Polym. J.,* 2007, **16,** 521-527.

14. R. van Dijkhuizen-Radersma, F. L. A. M. A. Peters, N. A. Stienstra, D. W. Grijpma, J. Feijen, K. de Groot and J. M. Bezemer, *Biomaterials,* 2002, **23,** 1527-1536.

15. Bhattacharyya, S.; Guillot, S.; Dabboue, H.; Tranchant, J. F.; Salvetat, J. P. *Biomacromolecules,* **2008,** *9,* 505.

16. A. K. Anal, *Recent Pat. Endocr. Metab. Immune Drug Discov.,* 2006, **1,** 83-90.

17. P. J. F. Harris, *Carbon nanotubes and related structures: new materials for the twenty-first century,* Cambridge University Press, United Kingdom, 1st edn., 1999, pp. 170-171.

18. J. P. Salvetat, Understanding of carbon nanotubes, Germany: Springer-Verlag Berlin Heidelberg, 1st edn., 2006, pp. 153-162.

19. A. Pourjavadi and G. R. Mahdavinia, *Turk. J. Chem.,* 2006, **30,** 595–608.

20. M. Boruah, M. Mili, S. Sharma, B. Gogoi and S. K. Dolui, *Polym. Compos.,* 2014, DOI:10.1002/pc.22909.

21. A. Pourjavadi and M. Doulabi, *Solid State Ionics,* 2014, **257,** 32–37.

22. S. Murdan, *J. Controlled Release,* 2003, **92,** 1–17

23. K. Sawahata, M. Hara, H. Yasunaga and Y. Osada, *J. Controlled Release,* 1990, **14,** 253-262.

UTILIZATION CERTIFICATE

FY 2015-2016

Certified that sum of Rs.2,37,334/- sanctioned during 1/04/2015 to 8/10/2015 of grant-in-aid amount in favour of Tezpur University vide DRDO letter No ERIP/ER/1103999M/01/1441 dated 24 March 2015, and Rs.2,37,334/- is released vide Latter No.ERIP/ER/1103999/M/01/1441 dated. 23/01/15 and amount of Rs. NIL is an interest earned(if any) from grants during the year whereas Rs.5,08,110/- on account of unspent balance of the previous year, a sum of Rs. 6,18,036/-has been utilized for the purpose for which it was sanctioned and that the balance of Rs. 1,27,408/-remaining unutilized is returned herewith vide DD no.....dated.....of Rs...1,27,408/-.

Signature of

Principal Investigator

18/11/15

Signature of 19.11.15

Accounts/Finance Officer

Finance Officer
Tezpur University

2.Certified that I have satisfied myself that the conditions on which the grants-in-aid was sanctioned have been fulfilled/are being fulfilled and that I have exercised the following checks to see that the money was actually utilized for the purpose for which it was sanctioned.

Kinds of checks exercised.

1

2

3

Counter signed by

Administrative Authority

(Designation with seal)

Registrar
Tezpur University

For SURAJIT CHAKRABORTY & CO.
CHARTERED ACCOUNTANTS

05-12-2015

CA. SURAJIT CHAKRABORTY
(Proprietor)
Membership No.- 305064

STATEMENT OF EXPENDUTURE ACCOUNTS

FOR THE FINANCIAL YEAR 2015-16

(a)Title of the project: "Development of Stimuli Responsive Polymeric Hydrogels and Their Applications"

(b)Sanction letter no& date: ERIP/ER/1103999M/01/1441

(c)Principal investigator: Prof. S. K. Dolui

(d)Date of Start of the Project: 9/10/2012

(e)Total Sanctioned cost of the project: Rs.28.29 Lakhs

(f)Grant received (Rs.) in 1yr.....13,83,000/-.....II yr.....6,73,372/-....III yr..4,95,947/-....iv yr 2,37,334/-

(g)Total Grant received so far: RS.27,89,653/-

Sl No.	Sanctioned Heads	Funds received for the year Rs.	Carried forward from Previous year Rs.	Funds available (i+ii) Rs.	Expenditure During 1/4/2015 To 31/10/2015 Rs.	Balance iii-iv Rs.
		i	ii	iii	iv	v
(a)	Staff	2,37,334/-	3,05,667/-	5,43,001/-	4,64,826/-	78,175/-
(b)	Equipment	NIL	NIL	NIL	NIL	NIL
(c)	Operation & Maint.	NIL	NIL	NIL	NIL	NIL

(d)	Expendables	NIL	26,984/-	26,984/-	NIL	26,984/-
(e)	Travel	NIL	39,147/-	39,147/-	15,914/-	23,233/-
(f)	Contingencies	NIL	30,000/-	30,000/-	30,984/-	(-)984/-
(g)	Research Consultant	NIL	NIL	NIL	NIL	NIL
(h)	Procured Service	NIL	NIL	NIL	NIL	NIL
	Institutional over head	NIL	1,06,312/-	1,06,312/-	1,06,312/-	NIL
	Interest earned, if any	NIL	NIL	NIL	NIL	NIL
	TOTAL	2,37,334/-	5,08,110/-	7,45,444/-	6,18,036/-	1,27,408/-

18/11/15

Name and Signature of
Principal Investigator
Date

19 Nov 15

Name and Signature of
Accounts Officer
Date:
Finance Officer
Tezpur University

Signature of Administrative Head
Registrar
Date: Tezpur University

For SURAJIT CHAKRABORTY & CO.
CHARTERED ACCOUNTANTS
05.12.2015
CA. SURAJIT CHAKRABORTY
(Proprietor)
Membership No.- 305054